

# 13

## One-particle inclusive transverse single-spin asymmetries

One of the most interesting and challenging issues at the moment concerns the question of asymmetries involving either an initial transversely polarized hadron, in which case we consider the analysing power  $A_N$  of the reaction, or the production of a transversely polarized final state hadron in an unpolarized collision, in which case we consider the polarizing power  $P$  of the reaction.

The problem is that the *lowest-order* QCD partonic cross-sections yield  $A_N = P = 0$ , whereas experimentally there is a mass of data showing large asymmetries or large polarizations, both in elastic and semi-inclusive reactions.

The treatment of elastic reactions is very different from that of the semi-inclusive case, requiring consideration of hadronic *wave functions* rather than parton densities. We shall therefore deal with the elastic case separately in Chapter 14.

The most dramatic examples in the one-particle inclusive case are the transverse asymmetries  $A_N$  in proton–proton and in antiproton–proton collisions ( $pp^\uparrow \rightarrow \pi^\pm X$  and  $\bar{p}^\uparrow p \rightarrow \pi^\pm X$ ) and the hyperon polarization in  $pp, p + \text{nucleus}$  and  $Kp \rightarrow \text{hyperon} + X$ .

Broadly speaking the effects have the following characteristics.

- (1) They increase linearly with  $p_T$  out to  $p_T \approx 2\text{--}2.5$  GeV/ $c$  (see Figs. 13.1, 13.2) though there is a hint of a flattening out beyond  $p_T \approx 1$  GeV/ $c$  in the lower energy data (see Fig. 13.3).
- (2) They increase linearly with Feynman  $x_F$  ( $x_F > 0$ ) out to the maximum  $x_F^{\text{max}} \approx 0.9$  (see Figs. 13.4 and 13.5).
- (3) They seem to be roughly energy-independent (see Fig. 13.2).
- (4) There are interesting dependences on the charge and strangeness of the final state hadron (see Fig. 13.6) and upon the correlation between the quark contents of the initial and produced hadrons.

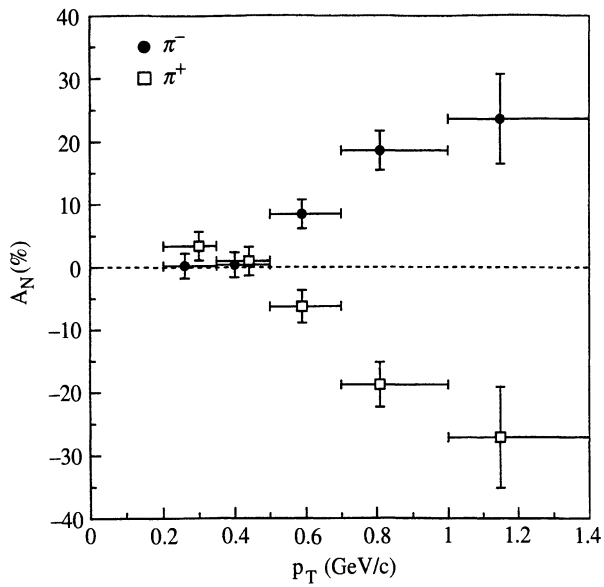


Fig. 13.1 Analysing power  $A_N$  vs.  $p_T$  measured at FERMILAB for 200 GeV/c polarized antiprotons in the reaction  $\bar{p}^\uparrow p \rightarrow \pi^\pm X$ . (From Bravar *et al.*, 1996.)

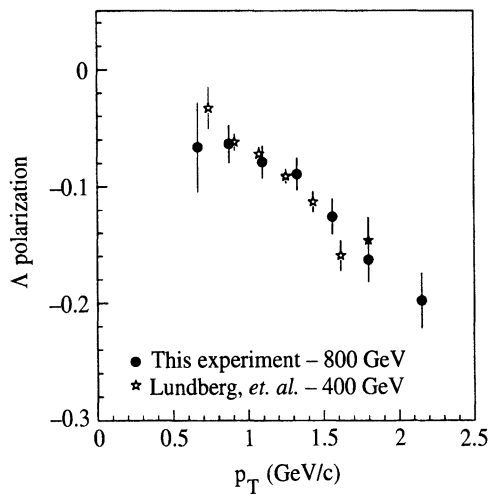


Fig. 13.2 The average  $\Lambda$  polarizations vs.  $p_T$  measured at FERMILAB for 800 GeV/c protons in the reaction  $pBe \rightarrow \Lambda X$  (from Ramberg *et al.*, 1994). Also shown are the 400 GeV/c data of Lundberg *et al.*, 1989.

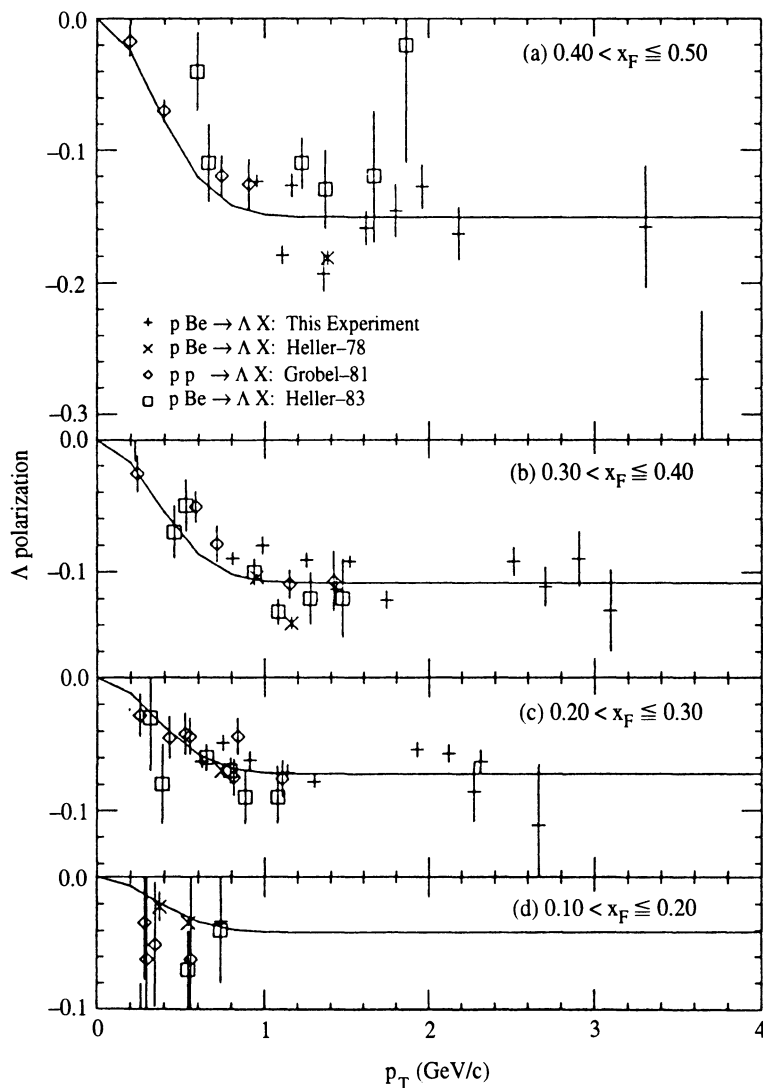


Fig. 13.3 The  $\Lambda$  polarization vs.  $p_T$  in bins of  $x_F$  measured at FERMI-LAB for 400 GeV/c protons in the reaction  $pBe \rightarrow \Lambda X$ . (From Lundberg *et al.*, 1989.)

### 13.1 Theoretical approaches

If one takes the same approach theoretically as was done for the asymmetries discussed in the previous chapter, i.e. a simple parton approach refined by QCD corrections with a perturbative QCD amplitude for the hard scattering, one can generate transverse asymmetries only by going

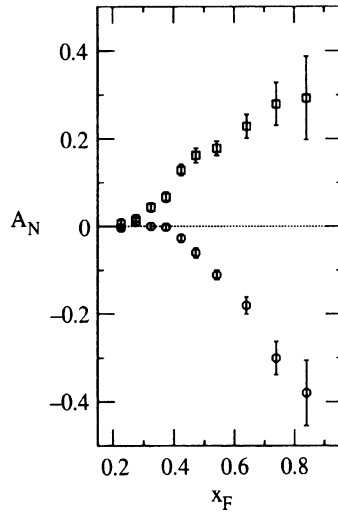


Fig. 13.4 Analysing power  $A_N$  vs.  $x_F$  measured at FERMILAB for 200 GeV/c polarized protons in the reaction  $p^\uparrow p \rightarrow \pi^\pm X$ :  $\square$ ,  $\pi^+$ ;  $\circ$ ,  $\pi^-$ . (From Adams *et al.*, 1991b.)

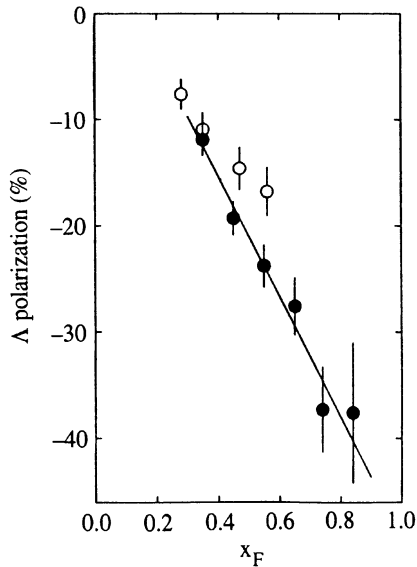


Fig. 13.5 The  $\Lambda$  polarization for  $p_T \geq 0.96$  GeV/c vs.  $x_F$  measured at CERN for the reaction  $pp \rightarrow \Lambda X$  at  $\sqrt{s} = 62$  GeV (solid circles) (from Smith *et al.*, 1987). Also shown (open circles) are the FERMILAB data at  $\sqrt{s} = 27$  GeV of Lundberg *et al.*, 1989.

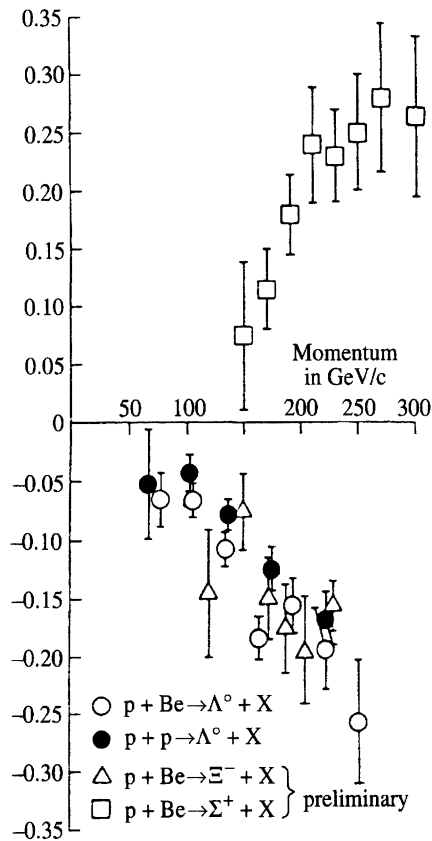


Fig. 13.6 Polarization of various hyperons produced by 400 GeV/c protons at FERMILAB at fixed Lab angle of 5 mrad. (From Heller, 1981.)

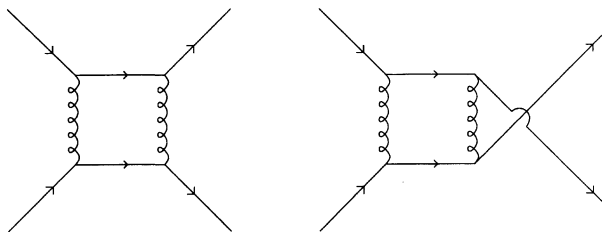


Fig. 13.7. Feynman diagram for quark-quark scattering amplitude at order  $\alpha_s^2$ .

beyond the Born approximation in the partonic amplitude. Thus at one-loop level, as shown for example in Fig. 13.7 for  $qq \rightarrow qq$ , one finds a non-zero value for  $\hat{a}_N$ , the partonic analogue of  $A_N$ , but it is exceedingly small, much too small to explain the data and moreover is proportional

to the quark mass. It has the typical form

$$\hat{a}_N = \alpha_s \frac{m_q}{\sqrt{s}} f(\theta^*). \quad (13.1.1)$$

This is similar to the problem of  $g_2(x)$  in polarized deep inelastic scattering (see Section 11.4) and really signals the failure of the model to produce the asymmetry. In our discussion of  $g_{1,2}(x)$  we followed the traditional approach using the hadronic and partonic tensors  $W_{\mu\nu}$  and  $w_{\mu\nu}$ ; however, we could have treated the asymmetries in terms of cross-section asymmetries in the  $eq \rightarrow eq$  partonic collision and would have found that the partonic asymmetry is zero for transverse polarization of the quark in the transversely polarized nucleon. Put another way, (13.1.1) indicates that the asymmetry is not a leading twist effect. Most interestingly, we shall see that the field-theoretic mechanism needed to discuss  $g_2(x)$  also provides a mechanism for a non-zero  $\hat{a}_N$ .

There are two diverse attitudes to the above situation. One point of view is that  $p_T$  is simply too small to justify the use of perturbative QCD, so one should try to construct phenomenological models for the non-perturbative aspects of the problem. We shall briefly examine this approach in Section 13.5. The alternative, which we shall follow, is to remain within the framework of the standard QCD-parton model but either to adopt a more sophisticated approach to the non-perturbative elements, i.e. the parton densities and the process of parton fragmentation (Sections 13.2, 13.3), or to generalize the partonic reactions beyond the usual  $2 \rightarrow 2$  Born amplitudes (Section 13.4).

Before discussing this it is important to note a major distinction between semi-inclusive lepton-hadron deep inelastic scattering and one particle inclusive hadron-hadron scattering, concerning the measurement of the analysing power  $A_N$  of the reaction.

In a hadron-hadron collision  $AB^\dagger \rightarrow CX$ , with  $OZ$  along the collision axis in the  $CM$ , we know from Sections 5.4 and 5.8 that the differential cross-section depends upon the azimuthal angle  $\phi$  of  $C$ , measured with respect to the quantization plane containing  $OZ$  and the transverse spin polarization  $\mathcal{P}_T$ .  $A_N$  can then be measured either by studying the azimuthal dependence with fixed  $\mathcal{P}_T$  or by studying the asymmetry when  $\mathcal{P}_T$  is reversed. The key point is that for an *unpolarized* collision there cannot be any dependence on an azimuthal angle about  $OZ$  – there simply is no physically defined plane from which to measure the angle.

The latter is not true for a reaction like  $ep \rightarrow e'CX$ . Even with unpolarized initial particles there can, in principle, be an azimuthal dependence about the ‘ $\gamma$ ’-proton  $CM$  collision axis, since in this frame  $\mathbf{p}(e)$  and  $\mathbf{p}(e')$  define a plane from which the angle can be measured. This cannot occur in the simple parton model, where partons are *collinear* with the momenta

of their parent hadrons and partons fragment collinearly into hadrons. But it can happen, for example, if one allows partons to have an intrinsic  $\mathbf{p}_T$  (Cahn, 1978). The azimuthal dependence arises in the following way. Consider the partonic electron–quark reaction  $eq(\mathbf{p}) \rightarrow e'q'(\mathbf{p}')$  in the ‘ $\gamma$ ’–proton CM, where  $\gamma$  has momentum  $\mathbf{q}$  along  $OZ$ . Since  $\mathbf{p}' = \mathbf{p} + \mathbf{q}$  we have that  $\mathbf{p}'_T = \mathbf{p}_T$ . Moreover the Mandelstam variables  $\hat{s}, \hat{t}, \hat{u}$  of the partonic reaction depend upon  $\phi$ , the azimuthal angle of  $\mathbf{p}_T$ , and hence the cross-section depends on the azimuthal angle of the final parton and therefore of  $C$ . Such azimuthal dependence is indeed seen experimentally (Arneodo *et al.*, 1987) and implies that  $A_N$  can only be measured by measuring an asymmetry under reversal of  $\mathcal{P}_T$ .

One final general comment is necessary. *All* the mechanisms we shall discuss are able to produce asymmetries that increase with transverse momentum, but they are able to do this only out to values  $\approx 1\text{--}2$  GeV/ $c$ . Beyond this the asymmetries decrease and eventually vanish. If, therefore, the experimental asymmetries continue to grow with  $p_T$  we shall find ourselves in a critical state of ignorance.

### 13.2 Standard QCD-parton model with soft-physics asymmetries

In this section we discuss a standard parton-model approach, with the hard scattering controlled by a  $2 \rightarrow 2$  partonic reaction but with allowance for transverse momentum of the partons. It will be seen that a transverse single-spin asymmetry could arise from possible asymmetries in the soft-physics aspects, i.e. in the parton number densities and fragmentation functions.

Consider the reaction

$$A^\uparrow + B \rightarrow C + X \tag{13.2.1}$$

where the momentum of  $A$  lies along  $OZ$  in the CM of the reaction;  $A$  is polarized transversely with spin along ( $\uparrow$ ) or opposite ( $\downarrow$ ) to  $OY$ .

Let us consider the cross-section for (13.2.1) in the spirit of the simplified analysis in Section 12.1. Since  $B$  is unpolarized here, it plays a passive rôle in the spin dependence, so we show only the rôle played by the partons in  $A$  and  $C$ . Then symbolically

$$d\sigma^\uparrow \sim f_\uparrow^\uparrow \hat{\sigma}_\uparrow D(\mathcal{P}_c) + f_\downarrow^\uparrow \hat{\sigma}_\downarrow D(-\mathcal{P}_c) \tag{13.2.2}$$

where  $f_\uparrow^\uparrow, f_\downarrow^\uparrow$  are the number densities of quarks with polarization  $\uparrow$  or  $\downarrow$  in  $A$ ,  $\hat{\sigma}_\uparrow, \hat{\sigma}_\downarrow$  are the lowest order cross-sections for the partonic reaction

$$(a^\uparrow \text{ or } a^\downarrow) + b \rightarrow c + d \tag{13.2.3}$$

and  $\pm\mathcal{P}_c$  is the spin-polarization vector of parton  $c$  produced in the reaction (13.2.3) when the polarization vector of  $a$  is  $\mathcal{P}_a = \pm\hat{e}_{(y)}$ .  $D(\mathcal{P}_c)$  is

the fragmentation function for

$$c(\mathcal{P}_c) \rightarrow C + X.$$

Now since  $\hat{a}_N = 0$  in lowest order, we have that

$$\hat{\sigma}_\uparrow = \hat{\sigma}_\downarrow = \hat{\sigma}. \tag{13.2.4}$$

Therefore (13.2.1) can be written

$$\begin{aligned} d\sigma^\uparrow &\sim \frac{1}{2} (f_\uparrow^\uparrow + f_\downarrow^\uparrow) \hat{\sigma} [D(\mathcal{P}_c) + D(-\mathcal{P}_c)] \\ &\quad + \frac{1}{2} (f_\uparrow^\uparrow - f_\downarrow^\uparrow) \hat{\sigma} [D(\mathcal{P}_c) - D(-\mathcal{P}_c)] \\ &= f^\uparrow \hat{\sigma} D + \frac{1}{2} (\Delta_T f) \hat{\sigma} \tilde{\Delta} D(\mathcal{P}_c) \end{aligned} \tag{13.2.5}$$

where  $f^\uparrow$  is simply the number density inside  $A^\uparrow$ ,  $D$  is the unpolarized fragmentation function

$$D = \frac{1}{2} [D(\mathcal{P}_c) + D(-\mathcal{P}_c)], \tag{13.2.6}$$

the difference  $\Delta_T f$  is given by

$$\Delta_T f \equiv f_\uparrow^\uparrow - f_\downarrow^\uparrow \tag{13.2.7}$$

and

$$\tilde{\Delta} D(\mathcal{P}_c) \equiv D(\mathcal{P}_c) - D(-\mathcal{P}_c). \tag{13.2.8}$$

Similarly

$$d\sigma^\downarrow \sim f^\downarrow \hat{\sigma} D - \frac{1}{2} (\Delta_T f) \hat{\sigma} \tilde{\Delta} D(\mathcal{P}_c).$$

In relation to the spin asymmetry we then have

$$\Delta_N d\sigma \equiv d\sigma^\uparrow - d\sigma^\downarrow \approx (\tilde{\Delta}_N f) \hat{\sigma} D + (\Delta_T f) \hat{\sigma} \tilde{\Delta} D(\mathcal{P}_c) \tag{13.2.9}$$

where

$$\tilde{\Delta}_N f \equiv f^\uparrow - f^\downarrow \tag{13.2.10}$$

and the asymmetry is defined as

$$A_N = \frac{d\sigma^\uparrow - d\sigma^\downarrow}{d\sigma^\uparrow + d\sigma^\downarrow} = \frac{\Delta_N d\sigma}{2d\sigma}. \tag{13.2.11}$$

Now the problem is that the expression (13.2.9) vanishes in the usual parton model, where the momentum of a parton is taken as *collinear* with the momentum of its parent hadron! Thus the total number of partons with momentum fraction  $x$  cannot depend on the polarization of the parent hadron, so that  $\tilde{\Delta}_N f = 0$ , and the total number of hadrons with momentum  $z\mathbf{p}_c$  cannot depend upon the polarization of  $c$ , so that  $\tilde{\Delta} D(\mathcal{P}_c) = 0$ .

It has been suggested, however, that with the inclusion of intrinsic parton transverse momentum these differences of number densities could be non-zero.

Thus Siverson (1990, 1991) proposed, for a hadron  $A$  that is transversely polarized,

$$f_a^A(\mathbf{p}_A, \mathcal{P}_A; x_a, \mathbf{k}_{aT}) = f_a^A(x_a, k_{aT}) + \frac{1}{2} \tilde{\Delta}_N f_a^A(x_a, k_{aT}) \frac{\mathcal{P}_A \cdot (\mathbf{p}_A \times \mathbf{k}_{aT})}{|\mathbf{p}_A \times \mathbf{k}_{aT}|} \quad (13.2.12)$$

where  $\mathbf{k}_{aT}$  is transverse to  $\mathbf{p}_A$ .

However, if we are permitted to regard  $f_a^A$  as describing the independent physical reaction

$$A(\mathbf{p}_A, \mathcal{P}_A) \rightarrow a(x_a \mathbf{p}_A + \mathbf{k}_{aT}) + X \quad (13.2.13)$$

then the asymmetry in the decay distribution implied by (13.2.12) is impossible, as can be seen by looking at the reaction in the CM of  $a$  and  $X$ . Collins (1993) has given a more subtle argument against the Siverson effect. Using the field-theoretic formalism of Section 11.9,  $\tilde{\Delta}_N f$  can be related to a nucleon matrix element of certain operators and is shown to vanish as a consequence of parity invariance and time-reversal invariance. But this argument relies on an absence of final state interactions and is thus analogous to treating (13.2.13) as an independent physical reaction, which is an essential element of the factorization of the reaction into universal soft and hard parts.

Despite these arguments, some authors have postulated a non-zero Siverson mechanism (Anselmino, Boglione, Murgia, 1995; Ratcliffe, 1998) on the grounds that the parton model totally ignores the question of the need to neutralize colour and to compensate for fractional charge and baryon number. So there must indeed be final state interactions, negating the anti-Siverson argument, but they must be fairly negligible otherwise the parton model would not work at all. In the papers quoted above there is no attempt to define the dynamics causing the final state interactions, so there is no reason to believe that a treatment relevant to one particular reaction is also relevant to any other process.

It turns out, in fact, that by extending the scope of the partonic reactions one can produce effective initial and final state interactions at the partonic level in a well-defined and factorizable dynamical way, as will be explained in Section 13.4. Thus we shall not discuss the Siverson mechanism any further.

Collins (1993) argued that, contrary to what happens in the Siverson case, the time-reversal argument does not forbid a non-zero  $\tilde{\Delta}D(\mathcal{P}_c)$  when  $\mathbf{k}_T$  is taken into account. He thus postulates, for the fragmentation process

$$c(\mathbf{p}_c, \mathcal{P}_c) \rightarrow C(z \mathbf{p}_c + \mathbf{k}_{cT}) + X \quad (13.2.14)$$

where  $\mathbf{k}_{CT}$  is perpendicular to  $\mathbf{p}_c$ ,

$$D(\mathbf{p}_c, \mathcal{P}_c; z\mathbf{p}_c + \mathbf{k}_{CT}) = D(z, k_{CT}) + \frac{1}{2}\Delta D(z, k_{CT})\mathcal{P}_c \cdot \frac{\mathbf{p}_c \times \mathbf{k}_{CT}}{|\mathbf{p}_c \times \mathbf{k}_{CT}|} \quad (13.2.15)$$

so that  $\tilde{\Delta}D(\mathcal{P}_c) \neq 0$ .

Since the Collins mechanism relies on detection of the produced hadron  $C$ , it will not be operative in jet production. Suggestions on the use of various reactions to try to sort out what mechanisms are at work are given in Anselmino, Leader and Murgia (1997) and in Boros, Liang, Meng and Rittel (1998).

How large are the asymmetries expected to be? If  $p_T$  is the magnitude of the transverse component of  $\mathbf{p}_C$  and  $\langle k_T \rangle$  is a measure of the magnitude of the intrinsic  $\mathbf{k}_T$ , we would expect effects of the order of  $\langle k_T \rangle / p_T$ . This is, of course, a higher-twist effect at large  $p_T$ .

Let us now consider the detailed expression for the asymmetry due to the Collins effect. For concreteness we shall consider the reaction

$$p^\uparrow + p \rightarrow \pi + X \quad (13.2.16)$$

at large  $p_T$ .

### 13.3 Collins mechanism for single-spin asymmetry

We consider the asymmetry arising from the second term in (13.2.9). The CM frame for the reaction  $p^\uparrow p \rightarrow \pi X$  is chosen so that the reaction takes place in the  $XZ$ -plane, with the polarized proton,  $A$ , moving along  $OZ$ . We consider pions whose momentum lies in the positive  $XZ$ -quadrant. The pion momentum is specified by  $p_{\pi T} (= p_{\pi x})$  and  $x_F = 2p_{\pi z} / \sqrt{s}$ .

The polarization direction  $\uparrow$  is defined to be along  $OY$ . The partons from the polarized proton have momentum  $x_a \mathbf{p}$  and those from the unpolarized proton have momentum,  $-x_b \mathbf{p}$ , where  $\mathbf{p}$  is the CM momentum of  $A$ .

Since intrinsic partonic  $\mathbf{k}_T$  effects are small we have taken them to be zero except where they are essential, i.e. in the fragmentation process.

Let quark  $c$  be produced at polar angles  $\theta^*, \phi^*$  in the partonic CM. The components of the polarization vector of  $c$ , with respect to the axes  $X_c, Y_c, Z_c$  in the helicity frame of  $c$  reached from the partonic CM (see Fig. 13.8), can be obtained from (5.6.20) together with (5.6.1), bearing in mind that the analysing power of the partonic reaction is zero. When the polarization vector of  $a$  is

$$\mathcal{P}_a = \mathbf{e}_{(y)} \quad (13.3.1)$$

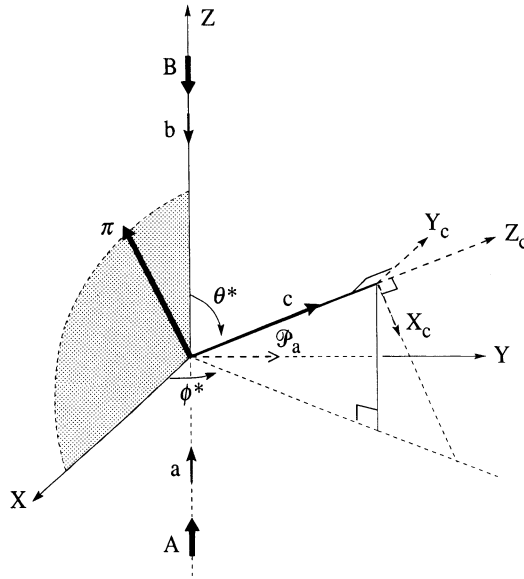


Fig. 13.8 Helicity frame for quark  $c$  reached from the parton CM in the reaction  $ab \rightarrow cd$ .

one has

$$\mathcal{P}_{x_c}^c \frac{d\hat{\sigma}(\mathcal{P}_a)^{ab \rightarrow cd}}{\hat{d}\hat{t}d\phi^*} = \left( \frac{1}{2\pi} \frac{d\hat{\sigma}}{\hat{d}\hat{t}} \right) (X0|X0) \sin \phi^* \tag{13.3.2}$$

$$\mathcal{P}_{y_c}^c \frac{d\hat{\sigma}(\mathcal{P}_a)^{ab \rightarrow cd}}{\hat{d}\hat{t}d\phi^*} = \left( \frac{1}{2\pi} \frac{d\hat{\sigma}}{\hat{d}\hat{t}} \right) (Y0|Y0) \cos \phi^*. \tag{13.3.3}$$

For all the relevant partonic processes one finds that

$$(X0|X0) = (Y0|Y0) \equiv \hat{d}_{NN}(\theta^*) \tag{13.3.4}$$

and also that  $d\hat{\sigma}(\mathcal{P}_a)/\hat{d}\hat{t}d\phi^*$  is independent of  $\phi^*$ . Hence (13.3.2) and (13.3.3) become

$$\mathcal{P}_{x_c}^c = \hat{d}_{NN}(\theta^*) \sin \phi^* \tag{13.3.5}$$

$$\mathcal{P}_{y_c}^c = \hat{d}_{NN}(\theta^*) \cos \phi^*. \tag{13.3.6}$$

From Fig. 13.8 one can read off the components of  $\mathcal{P}_c$  with respect to the partonic CM axes:

$$\mathcal{P}_x^c = \hat{d}_{NN}(\theta^*) [(\cos \theta^* - 1) \cos \phi^* \sin \phi^*] \tag{13.3.7}$$

$$\mathcal{P}_y^c = \hat{d}_{NN}(\theta^*) [\cos \theta^* \sin^2 \phi^* + \cos^2 \phi^*] \tag{13.3.8}$$

$$\mathcal{P}_z^c = -\hat{d}_{NN}(\theta^*) \sin \theta^* \sin \phi^*. \tag{13.3.9}$$

In fact one can see that  $\mathcal{P}_c$  is just the vector

$$\mathcal{P}_c = \hat{d}_{NN}(\theta^*) [\mathcal{R}(\theta^*)\mathbf{e}_{(y)}], \tag{13.3.10}$$

where  $\mathcal{R}(\theta^*)$  is the rotation about  $\mathbf{p}_a \times \mathbf{p}_c$  which takes  $\mathbf{p}_a$  into  $\mathbf{p}_c$ .

The expressions for  $\hat{d}_{NN}(\theta^*)$  are given in Table 13.1.

We can write eqns (13.3.7)–(13.3.9) as

$$\mathcal{P}_c = \hat{d}_{NN}(\theta^*)\mathbf{e} \tag{13.3.11}$$

where the unit vector  $\mathbf{e}$  is given by

$$\mathbf{e} = \left( (\cos \theta^* - 1) \cos \phi^* \sin \phi^*, \cos \theta^* \sin^2 \phi^* + \cos^2 \phi^*, -\sin \theta^* \sin \phi^* \right) \tag{13.3.12}$$

Let

$$\mathbf{p}_\pi = (\mathbf{p}_{\pi T}, p_{\pi z}) \tag{13.3.13}$$

and  $E_\pi$  be the momentum and energy of the produced  $\pi$  in the CM of the reaction. With our choice of axes,  $\mathbf{p}_{\pi T}$  lies along  $OX$ . Its momentum in the partonic CM is then

$$\mathbf{p}_\pi^* = (\mathbf{p}_{\pi T}, p_{\pi z}^*) \tag{13.3.14}$$

where

$$p_{\pi z}^* = \frac{1}{2\sqrt{x_a x_b}} [(x_a + x_b)p_{\pi z} - (x_a - x_b)E_\pi]. \tag{13.3.15}$$

Table 13.1. Partonic spin-transfer parameters

Reaction	$\hat{d}_{NN}$
$qq \rightarrow qq$	$\frac{-2\hat{s}\hat{u} \left(1 - \frac{\hat{t}}{3\hat{u}}\right)}{\hat{s}^2 + \hat{u}^2 + (\hat{s}^2 + \hat{t}^2)\frac{\hat{t}^2}{\hat{u}^2} - 2\hat{s}^2\frac{\hat{t}}{3\hat{u}}}$
$\bar{q}\bar{q} \rightarrow \bar{q}\bar{q}$	
$q\bar{q} \rightarrow q\bar{q}$	$\frac{-2\hat{s}\hat{u} \left(1 - \frac{\hat{t}}{3\hat{s}}\right)}{\hat{s}^2 + \hat{u}^2 + (\hat{u}^2 + \hat{t}^2)\frac{\hat{t}^2}{\hat{s}^2} - 2\hat{u}^2\frac{\hat{t}}{3\hat{s}}}$
$\bar{q}q \rightarrow \bar{q}q$	
$qq' \rightarrow qq'$	$\frac{-2\hat{s}\hat{u}}{\hat{s}^2 + \hat{u}^2}$
$q\bar{q} \rightarrow q'\bar{q}'$	
$\bar{q}q \rightarrow \bar{q}'q'$	
$qG \rightarrow qG$	
$\bar{q}G \rightarrow \bar{q}G$	

Now by the definition of  $\mathbf{p}_{\pi T}$  we can write

$$\mathbf{p}_\pi^* = z\mathbf{p}_c + \mathbf{k}_{\pi T} \tag{13.3.16}$$

where

$$\mathbf{k}_{\pi T} \cdot \mathbf{p}_c = 0 \tag{13.3.17}$$

so that

$$z = \frac{\hat{\mathbf{p}}_c \cdot \mathbf{p}_\pi^*}{p_c} \tag{13.3.18}$$

and

$$\mathbf{k}_{\pi T} = \mathbf{p}_\pi^* - (\hat{\mathbf{p}}_c \cdot \mathbf{p}_\pi^*)\hat{\mathbf{p}}_c. \tag{13.3.19}$$

Further, for the vector product needed in (13.2.15),

$$\mathbf{p}_c \times \mathbf{k}_{\pi T} = \mathbf{p}_c \times \mathbf{p}_\pi^* \tag{13.3.20}$$

so that  $\tilde{\Delta}D(\mathcal{P}_c)$  defined in (13.2.8) becomes, upon using (13.3.11) and (13.2.15),

$$\tilde{\Delta}D_\pi(\mathcal{P}_c) = \Delta D_\pi(z, k_{\pi T}) \hat{d}_{NN}(\theta^*) \frac{\mathbf{e} \cdot (\mathbf{p}_c \times \mathbf{p}_\pi^*)}{|\mathbf{p}_c \times \mathbf{p}_\pi^*|}. \tag{13.3.21}$$

Finally the cross-section difference (13.2.9) becomes

$$\begin{aligned} E_\pi \left( \frac{d^3\sigma^\uparrow}{d\mathbf{p}_\pi^3} - \frac{d^3\sigma^\downarrow}{d\mathbf{p}_\pi^3} \right) &= \sum_{a,b,c,d} \int dx_b f_b(x_b) \int dx_a \Delta_T f_a(x_a) E_\pi^* \\ &\times \int d\cos\theta^* \left[ \frac{d\hat{\sigma}^{ab \rightarrow cd}}{d\cos\theta^*} \right] \hat{d}_{NN}(\theta^*) \\ &\times \int \frac{d\phi^*}{2\pi} \Delta D_\pi(z, k_{\pi T}) \frac{\mathbf{e} \cdot (\mathbf{p}_c \times \mathbf{p}_\pi^*)}{p_c |\mathbf{p}_c \times \mathbf{p}_\pi^*|} \end{aligned} \tag{13.3.22}$$

where  $z$  and  $k_{\pi T}$  are given via (13.3.18) and (13.3.19),  $\mathbf{p}_\pi^*$  by (13.3.14) and (13.3.15) and  $\mathbf{e}$  by (13.3.12).

As suggested by Artru, Czyzewski and Yabuki (1997), we can get some feeling for the size of the effect if we note that at large  $x_F$  the dominant contribution comes from  $u$  and  $d$  quarks, for  $\pi^+$  and  $\pi^-$  respectively, and that the partonic scattering occurs predominantly at small  $\theta^*$ . In that case  $\hat{d}_{NN}(\theta^*) \approx 1$ ,  $\mathbf{p}_c$  is approximately along  $OZ$ ,  $\mathbf{k}_{\pi T} \approx \mathbf{p}_{\pi T} = p_{\pi T} \mathbf{e}$ , and  $\mathbf{e} \approx \mathbf{e}_{(y)}$ . The approximate asymmetry is then

$$A_{\pi^+N} \approx \frac{\Delta_T u(\bar{x})}{u(\bar{x})} \Delta D_\pi(\bar{z}, p_{\pi T}) \tag{13.3.23}$$

$$A_{\pi^-N} \approx \frac{\Delta_T d(\bar{x})}{d(\bar{x})} \Delta D_\pi(\bar{z}, p_{\pi T}) \tag{13.3.24}$$

where we have used isospin invariance for the fragmentation. Here  $\bar{x}$  and  $\bar{z}$  are the most probable values of  $x$  and  $z$  subject to  $\bar{x}\bar{z} \approx x_F$ . Equations (13.3.23) and (13.3.24) are essentially upper bounds to the magnitude of the asymmetry, since the angular integrations will dilute the effect.

From Fig. 13.4 one sees that  $A_{\pi^{\pm N}} \approx \pm 0.4$  for  $x_F \approx 0.8$ . Thus to produce the measured asymmetries entirely via the Collins mechanism requires firstly that

$$\frac{\Delta_T u(\bar{x})}{u(\bar{x})} \approx -\frac{\Delta_T d(\bar{x})}{d(\bar{x})}. \quad (13.3.25)$$

Given that for the longitudinal polarized-parton densities the measured values of  $\Delta u(x)/u(x)$  and  $\Delta d(x)/d(x)$  are in agreement with the sign, but not the magnitude, predicted using  $SU(6)$  wave functions for the nucleon, it is not unreasonable to expect to find the negative sign in (13.3.25), which follows from  $SU(6)$ , while finding that the magnitudes violate the  $SU(6)$  result

$$\frac{\Delta_T d(x)}{d(x)} = -\frac{1}{2} \frac{\Delta_T u(x)}{u(x)}. \quad (13.3.26)$$

Secondly, one requires

$$|\Delta D_\pi(\bar{z}, p_{\pi T})| \gtrsim \frac{0.4}{\min\{|\Delta_T u(\bar{x})/u(\bar{x})|, |\Delta_T d(\bar{x})/d(\bar{x})|\}} \quad (13.3.27)$$

Artru, Czyzewski and Yabuki (1997) parametrized  $\Delta D_\pi$ , using a model based on the Lund string and the simple *ansatz*

$$\frac{\Delta_T u(x)}{u(x)} = \frac{-\Delta_T d(x)}{d(x)} = \mathcal{P}_{\max} x^n \quad (13.3.28)$$

and found a best fit to the  $x_F$ -dependence of the data with  $\mathcal{P}_{\max} = 1$ ,  $n = 2$ . The factorized form  $F(z)G(k_T)$  involved is not compatible, however, with LEP DELPHI collaboration data (Abreu *et al.*, 1995a, b). This treatment is, of course, very approximate and recently Anselmino, Boglione, Hansson and Murgia (2000) have adopted a more systematic approach, with  $\Delta D_\pi$  parametrized as follows:

$$\Delta D_\pi(z, k_T) = N \frac{\langle k_T(z) \rangle}{M} z^\alpha (1-z)^\beta, \quad (13.3.29)$$

where the mean  $\langle k_T(z) \rangle$  is  $z$ -dependent and taken from the data of Abreu *et al.* (1995a, b) and  $N$ ,  $\alpha$ ,  $\beta$  are parameters to be fitted. For the transversely polarized quark densities it is assumed that  $\Delta_T d(x)/d(x)$  and  $\Delta_T u(x)/u(x)$  are both independent of  $x$ , with the  $SU(6)$  value

$$\frac{\Delta_T u(x)}{u(x)} = \frac{2}{3}. \quad (13.3.30)$$

The excellent fit to the data produces the surprising result

$$\frac{\Delta_T d(x)}{d(x)} = -1.33 \frac{\Delta_T u(x)}{u(x)}. \quad (13.3.31)$$

Now recall that, in the region where it is measured,  $\Delta d(x)$  is negative so that the very large value  $\Delta_T d(x)/d(x) \approx -8/9$  implied by (13.3.31) and (13.3.32) will violate the Soffer bound (11.9.18) over a significant range of  $x$ . In addition the positivity condition  $|\Delta D_\pi| \leq 2D_\pi$  is violated at large  $z$ . Thus the above treatment is inconsistent and must be disregarded.

An attempt at a consistent treatment by Boglione and Leader (2000) has led to some very surprising conclusions. The parametrizations of  $\Delta_T u(x)$ ,  $\Delta_T d(x)$  and  $\Delta D_\pi(z, k_T)$  are constructed so that both the Soffer bound and the positivity bound are automatically respected. However, in almost all parametrizations of  $\Delta d(x)$  obtained from fitting polarized DIS data,  $\Delta d(x)$  is negative for all  $x$ . As a consequence the Soffer bound

$$|\Delta_T d(x)| \leq \frac{1}{2} [d(x) + \Delta d(x)] \quad (13.3.32)$$

is highly restrictive. This leads to a conflict with the demand that  $|\Delta_T d(x)|$  be large in the region of large  $x$ , which is imposed by the fact that the  $\pi^\pm$  asymmetries are big, and of roughly equal magnitude, for large  $x_F$ . As

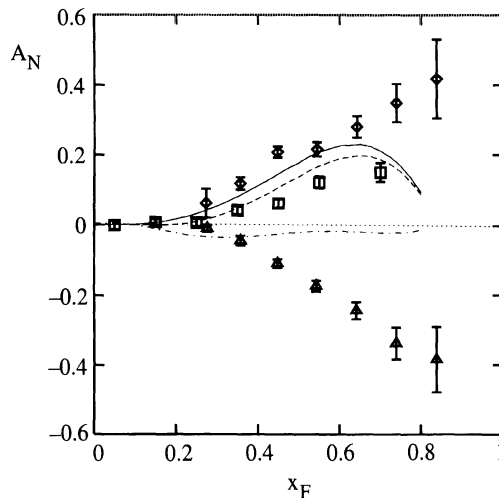


Fig. 13.9 The single-spin asymmetry  $A_N$  for pion production in  $p^\uparrow p \rightarrow \pi X$  as a function of  $x_F$  when using the GS polarized parton densities. The failure of the theory to fit the data can be seen. Solid line,  $\pi^+$ ; broken line  $\pi^0$ ; broken and dotted line  $\pi^-$ . (Courtesy of M. Boglione.)

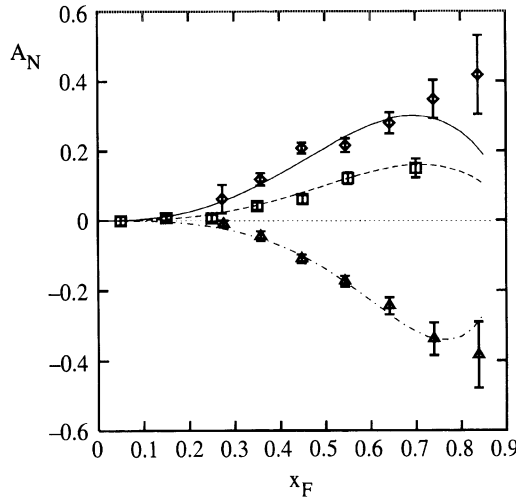


Fig. 13.10 The single-spin asymmetry  $A_N$  for pion production in the process  $p^\uparrow p \rightarrow \pi X$  as a function of  $x_F$ , obtained by using the BBS polarized parton densities in the Soffer bound. Solid line,  $\pi^+$ ; broken line,  $\pi^-$ ; broken and dotted line,  $\pi^0$ . (Courtesy of M. Boglione.)

an example, in Fig. 13.9 we show the very poor fit to the data when the GS polarized densities, due to Gehrmann and Stirling (1996), are used:  $\chi^2_{\text{DOF}} = 25!$  This raises an intriguing question. In (11.8.4) we pointed out that perturbative QCD arguments suggest that

$$\frac{\Delta q(x)}{q(x)} \rightarrow 1 \quad \text{as } x \rightarrow 1 \tag{13.33}$$

For the  $d$  quark this would imply that  $\Delta d(x)$  has to change sign and become positive at large  $x$ , thereby rendering the Soffer bound much less restrictive. In fact a more precise version of (13.33) is

$$\Delta q(x) = [1 - c(1 - x)^2] q(x) \quad \text{as } x \rightarrow 1 \tag{13.34}$$

where  $c$  is a positive constant. This is the origin of the fact that (13.33) is almost never imposed on  $\Delta q(x)$  when fitting data on polarized DIS, the point being that (13.34) is inconsistent with the evolution equations. In truth, however, one should not use the evolution equations near the exclusive region  $x = 1$ , so there is not really a contradiction. There are two fits to the polarized DIS data in the literature that do respect (13.34). The first, the BBS, due to Brodsky, Burkhardt and Schmidt (1995), is somewhat incomplete since  $Q^2$ -evolution was not used. The second, the (LSS)<sub>BBS</sub>, due to Leader, Sidorov and Stamenov (1998), uses the BBS parametrization but includes evolution. There is a dramatic improvement

to the fits to the  $\pi$  asymmetry data when these polarized densities are used, as seen in Figs. 13.10 and 13.11, which have  $\chi^2_{\text{DOF}}$ -values 1.45 and 2.41 respectively.

Note, however, that it does not seem possible to fit the asymmetry data at the largest values of  $x_F$ , indicating that the Collins mechanism alone is probably unable to explain all the  $\pi$  asymmetry data.

### 13.4 Beyond the standard QCD parton model

Consider once again, for concreteness, the reaction  $p_A^\uparrow p_B \rightarrow \pi X$ . Recall that the asymmetries are largest at large  $x_F$  and that these  $\pi^\pm$  are produced mainly from  $u$  and  $d$  quarks, respectively, having large values of  $x_a$  in the polarized proton and colliding with partons in the unpolarized proton with small values of  $x_b$ . We thus simplify by considering only valence quarks in  $p_A^\uparrow$  and gluons and antiquarks in  $p_B$ . To explain the approach we shall limit ourselves to one flavour of quark in  $p_A^\uparrow$  and of gluon in  $p_B$ .

The cross-section is proportional to the quantity  $W$  defined graphically in Fig. 13.12, where we do not show the fragmentation of the final quark  $q(p)$  into the pion. All final state particles, including the gluon but excluding  $q(p)$ , are summed over. In this diagram the soft physics is in

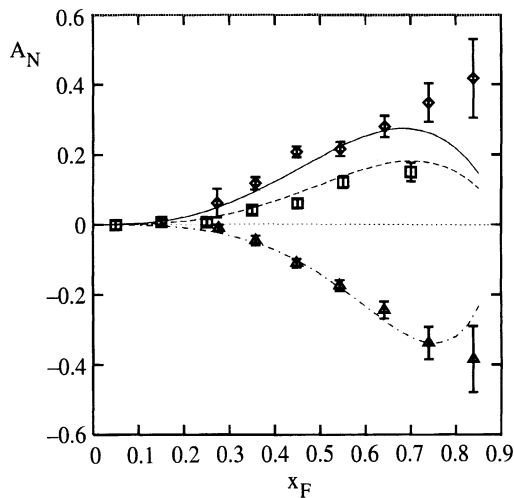


Fig. 13.11 The single-spin asymmetry  $A_N$  for pion production in the process  $p^\uparrow p \rightarrow \pi X$  as a function of  $x_F$ , determined by the fit using the  $(\text{LSS})_{\text{BBS}}$  polarized parton densities in the Soffer bound. Solid line,  $\pi^+$ ; broken line,  $\pi^0$ ; broken and dotted line,  $\pi^-$ . (Courtesy of M. Boglione.)

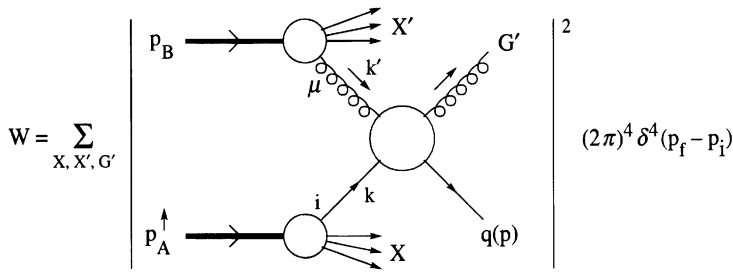


Fig. 13.12 Graphical definition of  $W$  for  $p^\uparrow p \rightarrow \pi X$  in the standard QCD-parton model.  $\mu$  is a Lorentz index,  $i$  a spinor index.

the amplitudes for  $p_A^\uparrow$  and  $p_B$  to split into partons, and the  $Gq \rightarrow G'q$  amplitude describes a hard process and is calculated in lowest-order perturbative QCD, i.e. using just the Born terms. Since the treatment of the *unpolarized* proton  $p_B$  is conventional, let us, to simplify the discussion, remove it and thus effectively consider

$$p_A^\uparrow + G \rightarrow \pi + X$$

and, to simplify even further, just consider one of the possible hard scattering Born terms, i.e. take

$$W = \sum_{X, G'} |M_q|^2 (2\pi)^4 \delta(p_f - p_i) \tag{13.4.1}$$

where  $M_q$  is shown in Fig. 13.13.

As in Section 11.5 the result for  $W$  can be written as a Feynman diagram with a cut propagator, in this case a gluon propagator, as shown in Fig. 13.14, with a similar structure to (11.5.14). Recall that the Collins mechanism for a transverse spin asymmetry came from the fragmentation

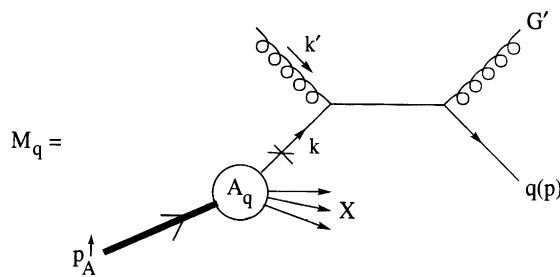


Fig. 13.13. Simplified version for  $M_q$  for the reaction  $p^\uparrow G \rightarrow \pi X$ . The cross on the fermion line indicates that there is no propagator for the quark of momentum  $k$ .

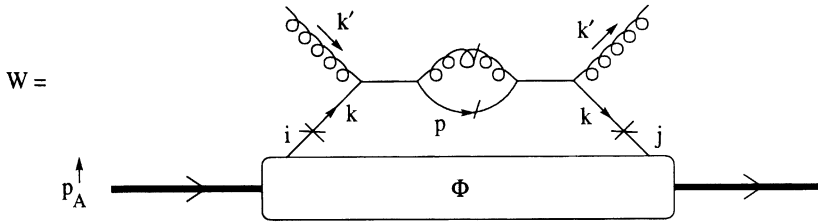


Fig. 13.14. Field-theoretic diagram corresponding to (13.4.1);  $i, j$  are spinor indices.

of  $q(p)$  into a pion with non-zero transverse momentum. Our diagram really corresponds to

$$p^\uparrow + G \rightarrow \text{jet} + X \tag{13.4.2}$$

so the Collins mechanism is inoperative. Also, if time reversal is an exact symmetry then the Siver's mechanism that places the asymmetry in the spin-dependent quark density is absent and, as stressed earlier, we are unable to produce an asymmetry. To remedy this, and for several other reasons as well, Efremov and Teryaev (1984), following ideas of Ellis, Furmanski and Petronzio (1983), introduced a correlated quark–gluon density function, which, as we shall see, does yield an asymmetry.

Consider the soft amplitude for a proton to produce a quark, a gluon of colour  $a$  and index  $\mu$  and some other set of particles  $X$ . To simplify the analysis pretend that  $X$  is fixed. The amplitude  $A_{qG}^{\mu,a}$  is a Dirac spinor (see Section 11.5), and is shown graphically in Fig. 13.15, where as usual there are no propagators for partons. Conventionally, if the quark has momentum  $k_1$  the gluon is given momentum  $k_2 - k_1$ . Combining the

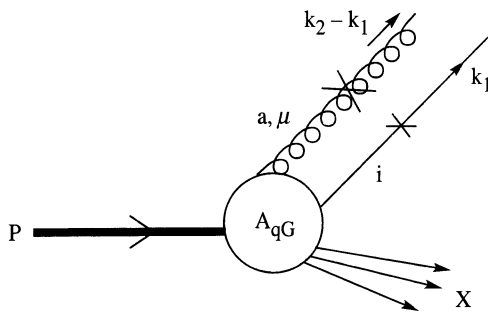


Fig. 13.15 The amplitude for a proton to produce a quark, a gluon and some set of particles  $X$ .





Since this is the colour structure that will always occur it is convenient to absorb the  $t_{sl}^a$  into the soft amplitude, and, by convention, for reasons that will appear clear later, a factor of the strong coupling  $g$ . Thus the operator structure in (13.4.5) becomes

$$\sum_a g \bar{\Psi}_j t^a A_\mu^a \Psi_i^l = \bar{\Psi}_j g A_\mu \Psi_i \tag{13.4.8}$$

where,  $A_\mu$  is the matrix

$$A_\mu = \sum_a t^a A_\mu^a \tag{13.4.9}$$

and  $\Psi_i$  is now a column vector in colour space.

Hence one utilizes the colour-singlet correlator

$$\begin{aligned} \Phi_{A_{ij}}^\mu(k_1, k_2; P, \mathcal{S}) &= \int \frac{d^4 y}{(2\pi)^4} \frac{d^4 z}{(2\pi)^4} e^{ik_1 \cdot z} e^{i(k_2 - k_1) \cdot y} \\ &\times \langle P, \mathcal{S} | \bar{\Psi}_j(0) g A^\mu(y) \Psi_i(z) | P, \mathcal{S} \rangle. \end{aligned} \tag{13.4.10}$$

Now the crucial point is that time-reversal invariance does not prohibit  $\Phi_A^\mu$  from having  $\mathcal{S}_T$ -dependent terms of the form

$$i b_V \epsilon^{\mu\alpha\beta\gamma} \mathcal{S}_\alpha P_\beta n_\gamma \not{P} + b_A \mathcal{S}^\mu \not{P} \gamma_5 \tag{13.4.11}$$

where  $b_V$  and  $b_A$  are *real* scalar functions and where  $n_\mu$  is the null vector fixing the gauge  $A^\mu n_\mu = 0$ ; see (11.5.24). Then, recalling that there is one  $\gamma$ -matrix at each vertex and in each fermion propagator (as usual, neglecting quark-mass terms), one sees that the hard part of Fig. 13.17 contains a product of seven  $\gamma$ -matrices. When the trace analogous to (11.5.14) is taken using  $\Phi_A$ , the  $b_V$  term in (13.4.11) will involve a trace of eight  $\gamma$ -matrices, which will be real, whereas the  $b_A$  term involves eight  $\gamma$ -matrices and also  $\gamma_5$  and will be imaginary. In consequence the traces over the terms in (13.4.11) produce a result proportional to  $i$ .

Next we count the factors of  $i$  coming from quark–gluon vertices and all non-cut propagators, both quark and gluon. There are seven of them, so that they yield a factor of  $i$ .

In total, then, we have a product of three factors  $i$ , from colour, from vertices and from the trace with the soft amplitude. Thus, contrary to our hope, the relevant spin-dependent part of the Feynman diagram in Fig. 13.17 appears to be imaginary.

However, in the loop integrations over  $k_1, k_2$  (and  $k'$  when the upper gluon is attached to a hadron) we encounter the point where the gluon propagator on the left, carrying momentum  $k_2 - k_1 + k'$ , is on shell, i.e. where  $(k_2 - k_1 + k')^2 = 0$ . As can be understood from eqn (11.5.12), this will give a term  $-i\pi\delta[(k_2 - k_1 + k')^2]$ , which just provides the last  $i$  necessary to render the amplitude real!

Finally, then, we have a mechanism for producing a single-transverse-spin asymmetry that respects all the fundamental discrete symmetries of QCD. The asymmetry is calculated from the Feynman diagram of Fig. 13.17, in which, in the propagator for the gluon carrying momentum  $k_2 - k_1 + k'$ , one makes the replacement

$$\frac{i}{(k_2 - k_1 + k')^2 + i\epsilon} \rightarrow \pi\delta \left[ (k_2 - k_1 + k')^2 \right]. \tag{13.4.12}$$

The final result takes a form analogous to (11.5.14):

$$I = \int d^4k_1 d^4k_2 \text{Tr} [\Phi_A^\mu S_\mu(k_1, k_2)] + \text{c.c.}, \tag{13.4.13}$$

where  $S_\mu$  is the short-distance amplitude with the modification (13.4.12) and a factor  $gt_{sl}^a$  removed.

The detailed analysis is exceedingly complicated (Qiu and Sterman, 1999) and the above pedagogical treatment aims only at presenting the essential ideas.

In a more careful treatment the following points should be noted.

- (1) The above discussion focussed on the pole in the gluon propagator and is referred to as the *gluonic pole mechanism*.
- (2) There are other diagrams involving  $\Phi_A^\mu$  that contribute to the asymmetry. An example is shown in Fig 13.19. In this case the extra factor  $i$  is produced via the pole in the fermion propagator carrying momentum  $k_1 + k'$ , i.e. at  $(k_1 + k')^2 = 0$ . This is referred to as the *fermionic pole mechanism* and has been studied by Efremov, Korotkiyan and Teryaev (1995), by Teryaev (1995) and by Korotkiyan and Teryaev (1995).
- (3) There is an unresolved dispute in the literature whether the gluon or fermion pole is expected to be the dominant mechanism. The kinematics are such that in the gluon pole case the gluon field in the proton corresponds to a static, constant, field. In the fermion pole case one has the somewhat strange concept of a static, constant, fermion

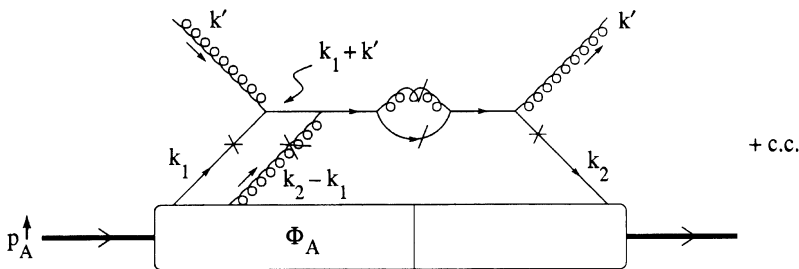


Fig. 13.19. Alternate type of interference term involving  $\Phi_A$ .

field. A complete treatment, including both mechanisms, has not, to our knowledge, been carried out for the reaction  $p^\uparrow p \rightarrow \pi X$ , but we shall give below the result for the simpler process  $p^\uparrow p \rightarrow \gamma X$ .

- (4) The above discussion involving 4-vectors  $k_{1,2}^\mu$  is, as in the discussion of Section 11.5, too general and is not yet in parton-model form. One still has to make the leading collinear approximation  $k_1 = x_1 P$ ,  $k_2 = x_2 P$  in the hard amplitude and then carry out the integration  $\int dk^- d^2 \mathbf{k}_T$  for both  $k_1$  and  $k_2$  in the soft amplitude. Thereby one comes finally to the standard form of correlator

$$\Phi_A^\mu(x_1, x_2; P, \mathcal{S}) = \int \frac{d\lambda}{2\pi} \frac{d\zeta}{2\pi} e^{i\lambda x_1} e^{i\zeta(x_2 - x_1)} \times \langle P, \mathcal{S} | \bar{\Psi}_j(0) A^\mu(\zeta n) \Psi_i(\lambda n) | P, \mathcal{S} \rangle \quad (13.4.14)$$

involving operators on the light-cone. (recall that  $n^2 = 0$ ).

- (5) Since we are studying a twist-3 contribution we must, for consistency, include the non-leading twist-3 terms coming from the standard parton diagram Fig. 11.7. These arise when one goes beyond the collinear approximation  $k = xP$  inside the hard amplitude  $S$  in the hadron-hadron analogue of (11.5.14). The inclusion of transverse momentum involves making a Taylor expansion of  $S(k)$  about the point  $k^\mu = xP^\mu$ :

$$S(k^\mu) = S(k^\mu = xP^\mu) + (k^\mu - xP^\mu) \frac{\partial}{\partial k^\mu} S(k^\mu) + \dots \quad (13.4.15)$$

and the term  $(k^\mu - xP^\mu) \Phi_{ij}$  can be transformed, via partial integration, into a matrix element involving  $\partial^\mu \Psi(z)$ . The beautiful, and perhaps unsurprising, result is that this term can be combined with  $\Phi_A^\mu$  to produce a new correlator

$$\Phi_{D_{ij}}^\mu(k_1, k_2; P, \mathcal{S}) = \int \frac{d^4 y}{(2\pi)^4} \frac{d^4 z}{(2\pi)^4} e^{ik_1 \cdot z} e^{i(k_2 - k_1) \cdot y} \times \langle P, \mathcal{S} | \bar{\Psi}_j(0) \vec{D}^\mu(y) \Psi_i(z) | P, \mathcal{S} \rangle \quad (13.4.16)$$

where

$$\vec{D}^\mu(y) \Psi_i(z) = \left[ i \frac{\partial \Psi_i(z)}{\partial z_\mu} + g A^\mu(y) \Psi_i(z) \right] \quad (13.4.17)$$

(the arrows indicate that the operator acts only to the right) is similar to the standard covariant derivative that appears in the QCD equation of motion

$$\left[ \vec{D}(z) - m_q \right] \Psi(z) = 0. \quad (13.4.18)$$

Finally, after making the collinear approximation in the twist-3 part involving  $A^\mu$ , the correlator involved becomes

$$\Phi_{D_{ij}}^\mu(x_1, x_2; P, \mathcal{S}) = \int \frac{d\lambda}{2\pi} \frac{d\zeta}{2\pi} e^{i\lambda x_1} e^{i\zeta(x_2-x_1)} \times \langle P, \mathcal{S} | \bar{\Psi}_j(0) \vec{D}^\mu(\zeta n) \Psi_i(\lambda n) | P, \mathcal{S} \rangle. \quad (13.4.19)$$

This is a very interesting approach and, although the basic idea is not new, it is only now that detailed calculations are beginning to be performed. It may well be that in combination with the Collins mechanism one can obtain a fit to all the data on the  $\pi$  asymmetry. However, it is clearly essential to study asymmetries in reactions where the Collins mechanism is inoperative, e.g. in hard  $\gamma$  or jet production, in order to learn more about the gluonic and fermionic pole mechanisms.

The reaction  $p_A^\dagger p_B \rightarrow \gamma X$  is the only case, to our knowledge, where the entire contribution of gluonic and fermionic poles has been taken into account (Qiu and Sterman, 1992) and the structure of their result is instructive.

Let the photon emerge with momentum  $\mathbf{p}_\gamma$  and energy  $E_\gamma$ . Then

$$E_\gamma \left( \frac{d^3\sigma(\mathcal{S}_T)}{d^3\mathbf{p}_\gamma} - \frac{d^3\sigma(-\mathcal{S}_T)}{d^3\mathbf{p}_\gamma} \right) = \frac{\alpha\alpha_s}{s} \epsilon_{\mu\nu\rho\sigma} \mathcal{S}_T^\mu p_\gamma^\nu n^\rho p_A^\sigma \int \frac{dx_b}{x_b} G(x_b) \int \frac{dx_a}{x_a} \delta(\hat{s} + \hat{t} + \hat{u}) \times \sum_f e_f^2 [G_f(x_a, x_b, p_\gamma) + F_f(x_a, x_b, p_\gamma)] \quad (13.4.20)$$

where  $G_f$  and  $F_f$  are the contributions of flavour  $f$  from gluonic ( $G$ ) and fermionic ( $F$ ) poles respectively,  $n^\mu$  is given in (11.5.24) and  $\hat{s}, \hat{t}, \hat{u}$  are the Mandelstam variables involved in the partonic process

$$\hat{s} = x_a x_b s \quad \hat{t} = x_a t \quad \hat{u} = x_b u. \quad (13.4.21)$$

In terms of quark–gluon correlators  $T$  and hard scattering terms  $H$  one has for the gluonic pole:

$$G_f = H_G^{(1)}(x_a, x_b, p_\gamma) T_G^{(V)}(x_a, x_a) + H_G^{(2)}(x_a, x_b, p_\gamma) \left[ T_G^{(V)}(x_a, x_a) - x_a \frac{\partial}{\partial x_a} T_G^{(V)}(x_a, x_a) \right] \quad (13.4.22)$$

where

$$H_G^{(1)} = -\frac{3g}{8} \left( \frac{1}{\hat{t}} \right) \quad (13.4.23)$$

and

$$H_G^{(2)} = \frac{3g}{8} \left( \frac{1}{\hat{u}} \right) \left( \frac{\hat{s}}{\hat{t}} + \frac{\hat{t}}{\hat{s}} \right). \quad (13.4.24)$$

The soft quark–gluon correlator  $T_G^{(V)}$  is real and is given by

$$T_G^{(V)} = n_\mu \epsilon_{\nu\alpha\beta\gamma} n^\alpha p_A^\beta \mathcal{S}_T^\gamma \int \frac{d\lambda d\xi}{4\pi} e^{i\lambda x} \langle p_A; \mathcal{S}_T | \bar{\Psi}(0) \not{G}^{\mu\nu}(\xi n) \Psi(\lambda n) | p_A; \mathcal{S}_T \rangle \quad (13.4.25)$$

where  $G^{\mu\nu}$  is the gluon field-strength tensor. For the fermionic pole one has

$$F_f = H_D^{(1)}(x_a, x_b, p_\gamma) \left[ T_D^{(V)}(0, x_a) + iT_D^{(A)}(0, x_a) \right] \quad (13.4.26)$$

where  $T_D^{(V)}$  is real,  $T_D^{(A)}$  pure imaginary. Here

$$H_D^{(1)} = \frac{1}{24} \left( \frac{9}{\hat{s}} - \frac{1}{\hat{t}} \right) \quad (13.4.27)$$

and the correlators are

$$T_D^{(V)}(0, x) = \epsilon_{\mu\alpha\beta\gamma} n^\alpha p_A^\beta \mathcal{S}_T^\gamma \int \frac{d\lambda d\xi}{4\pi} e^{i\lambda x} \langle p_A; \mathcal{S}_T | \bar{\Psi}(0) \not{D}^\mu(\xi n) \Psi(\lambda n) | p_A; \mathcal{S}_T \rangle \quad (13.4.28)$$

and

$$T_D^{(A)} = \mathcal{S}_T^\mu \int \frac{d\lambda d\xi}{4\pi} e^{i\lambda x} \langle p_A; \mathcal{S}_T | \bar{\Psi}(0) \not{\gamma}_5 D_\mu(\xi n) \Psi(\lambda n) | p_A; \mathcal{S}_T \rangle. \quad (13.4.29)$$

Qiu and Sterman (1999) argue that the correlators in the fermionic pole case are essentially the overlap of states in one of which the quark has momentum  $xp$  and in the other of which all this momentum is carried by the gluon, so that the overlap should be small. In the gluonic pole case, on the contrary, in both states the quark carries momentum  $xp$ , so that the overlap might be expected to be larger. For this reason Qiu and Sterman expect the gluonic pole mechanism to dominate. Further, they suggest that typically  $T_G^{(V)}(x, x)$  will vanish like  $(1-x)^\beta$  as  $x \rightarrow 1$  with  $\beta > 0$ , in which case the term  $x(\partial/\partial x)T_G^{(V)}(x, x)$  in (13.4.22) will dominate at large  $x$ . (In their treatment of  $p^\dagger p \rightarrow \pi X$  mentioned earlier, Qiu and Sterman keep just this term.)

In conclusion to this section, we note that the theoretical developments are fascinating, but it will be a mammoth task to sort out the mechanisms and learn experimentally about the various correlators.

### 13.5 Phenomenological models

It is a historical fact that we have known ever since 1976 that hyperons, and in particular  $\Lambda$ s, are produced in a highly polarized state in the high energy collision of unpolarized hadrons (Bunce *et al.*, 1976). A sample of the data was shown in Figs. 13.2, 13.3, 13.5 and 13.6. The general features were summarized at the beginning of Chapter 13.

In this section we shall briefly describe some of the phenomenological attempts to explain the hyperon data. None is really convincing, firstly because they are really semiclassical models, secondly because, while enjoying some success, they cannot account for all the main features of the data.

Concerning the semiclassical aspect there is an important point that should be noted. If, as is conventional, one works with helicity amplitudes, the asymmetry or polarization is always of the form

$$A \propto \text{Im} \left( \phi_{\text{flip}}^* \phi_{\text{non-flip}} \right) \quad (13.5.1)$$

where the  $\phi$  are helicity amplitudes involving either helicity-flip or no helicity-flip. Thus one requires a model for the *amplitudes* and their phases, a concept beyond classical physics.

To evade this dilemma one can work in a basis where the spin states are transverse, see Section 11.9 and one then finds that (13.5.1) is replaced by

$$A \propto |f_{\text{non-flip}}|^2 - |f_{\text{flip}}|^2 \quad (13.5.2)$$

where  $f$  are amplitudes involving either flip or non-flip of the transverse spin. In this formalism one *can* make a probabilistic model for the moduli squared of the amplitudes; however, such a theory can never be totally satisfactory because there will be in general other spin-dependent variables that *do* involve interference between the transverse spin amplitudes, and these will then be outside the scope of the model.

At the time of writing there seems to be some hope of attacking the matter in a more fundamental way, using an analogue of the Collins mechanism, discussed in Section 13.4, in which an unpolarized quark can fragment into a polarized hadron if  $p_T$  is non-zero. However, it would be premature to comment on this approach, so we shall outline some of the phenomenological methods used over the past two-and-a-half decades. Our presentation owes much to the review of Soffer (1999).

In very broad terms the following features, specific to the hyperon polarization, require explanation:

$$\mathcal{P}_\Lambda \sim \mathcal{P}_{\Xi^-} \sim \mathcal{P}_{\Xi^0} \quad (13.5.3)$$

$$\mathcal{P}_{\Sigma^+} \sim \mathcal{P}_{\Sigma^-} \sim -\mathcal{P}_\Lambda \quad (13.5.4)$$

$$\mathcal{P}_{\Lambda} \sim \mathcal{P}_{\Xi^0} \sim 0 \tag{13.5.5}$$

yet

$$\mathcal{P}_{\Sigma^-} \sim \mathcal{P}_{\Sigma^+} \quad \mathcal{P}_{\Xi^+} \sim \mathcal{P}_{\Xi^-}. \tag{13.5.6}$$

All our considerations will be directed at the beam fragmentation region where most of the data lie.

### 13.5.1 The Lund model

Consider  $pp \rightarrow \Lambda X$ , in which the  $\Lambda$  has transverse momentum  $p_T$ . The hadrons are assumed to have simple  $SU(6)$  three-quark wave functions. Thus the  $\Lambda$  consists of an isosinglet ( $ud$ ) diquark with spin  $S = 0$  and a strange quark, which carries the spin of the  $\Lambda$ . The reaction is visualized as follows (Andersson, Gustafson and Ingelman, 1979; Andersson *et al.*, 1983). A suitable  $ud$  diquark from the proton moves forward, stretching the confining colour field, which ultimately ‘snaps’, producing an  $s\bar{s}$  pair in a process that conserves angular momentum locally (see Fig. 13.20).

The momenta of the  $s$  and  $\bar{s}$  are chosen to allow the  $s$  to combine with the essentially forward-going  $ud$  to produce a  $\Lambda$  with  $p_T$  as indicated. In this configuration the  $s\bar{s}$  pair has orbital angular momentum along  $\mathbf{p} \times \mathbf{p}_{\Lambda}$ . To compensate for this, the spins  $s$  and  $\bar{s}$  must be along  $-(\mathbf{p} \times \mathbf{p}_{\Lambda})$ . Consequently the  $\Lambda$  emerges with polarization along  $-(\mathbf{p} \times \mathbf{p}_{\Lambda})$ , as is found experimentally.

For the production of  $\Sigma^0$ , the  $SU(6)$  wave function is built up from a  $ud$  diquark with  $S = 1$ . The two spin states of the  $\Sigma^0$ , referred to an axis along  $\mathbf{p} \times \mathbf{p}_{\Sigma}$ , are

$$\begin{aligned} |\tfrac{1}{2}\rangle &= \sqrt{\tfrac{2}{3}} |1; -\tfrac{1}{2}\rangle - \sqrt{\tfrac{1}{3}} |0; \tfrac{1}{2}\rangle \\ |-\tfrac{1}{2}\rangle &= \sqrt{\tfrac{1}{3}} |0; -\tfrac{1}{2}\rangle - \sqrt{\tfrac{2}{3}} |-1; \tfrac{1}{2}\rangle \end{aligned} \tag{13.5.7}$$

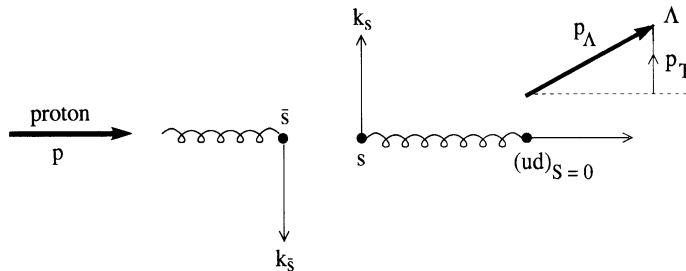


Fig. 13.20. Schematic diagram of the breaking of a Lund string to produce an  $s\bar{s}$  pair.

and since the  $s\bar{s}$  configuration that produces the required  $p_T$  has an  $s$  with spin projection  $1/2$  one sees easily that

$$\mathcal{P}_{\Sigma^0} = -\left(\frac{1}{3}\right)\mathcal{P}_{\Lambda}. \tag{13.5.8}$$

A similar result holds for  $\Sigma^+$ .

There seems to be only one measurement of  $\mathcal{P}_{\Sigma^0}$  and it is in agreement with the sign in (13.5.8). As seen in Fig. 13.6, the sign of  $\mathcal{P}_{\Sigma^+}$  is also in agreement with (13.5.8), but not the magnitude.

However, the mechanism for  $\Sigma^-$  production must be quite different, since the string-breaking must provide a  $ds$  pair. Nonetheless,  $\mathcal{P}_{\Sigma^-}$  is much like  $\mathcal{P}_{\Sigma^+}$ . It is equally unclear why  $\Xi^-$  and  $\Xi^0$  have the same polarization as the  $\Lambda$ .

Finally, the vanishing of the polarizations for  $\bar{\Lambda}$  and  $\bar{\Xi}^0$  seems intuitive since the entire particle has to be created via the string-breaking. But then the significant polarizations of the  $\bar{\Sigma}^-$  and the  $\bar{\Xi}^+$  are a mystery.

In short, while the model has some success it in no way provides an adequate quantitative description of the data.

### 13.5.2 The Thomas precession model

This very clever semiclassical model, due to De Grand and Miettinen (1981), utilizes the Thomas precession to argue in favour of a higher probability for particular states of polarization.

Here it is assumed that a  $u$  quark from the beam proton of momentum  $\mathbf{p}$  is wrenched off in the collision, leaving a fast forward-moving  $S = 0$   $ud$  diquark with momentum roughly  $\frac{2}{3}\mathbf{p}$  and various low-momentum sea partons; one of these, an  $s$ , is then attracted towards and binds with the  $ud$  to form the  $\Lambda$ . The  $s$  quark is assumed to have transverse momentum  $\mathbf{p}_T$ . It is further assumed that the force that drags it towards the forward-moving  $ud$  diquark arises from a Lorentz scalar potential.

The process by which the  $s$  and the  $ud$  come together is viewed in a hybrid fashion. Firstly, one pictures the classical orbits involved to argue that the orbital angular momentum  $\mathbf{L}$  of the  $s$  is opposite to  $\mathbf{p} \times \mathbf{p}_{\Lambda}$ . Next, one visualizes the interaction between the spinless  $ud$  and the spin- $1/2$   $s$  in quantum mechanical terms involving a scalar attractive potential  $V(r)$ . As explained in subsection 2.2.8 the Thomas precession induces a rotation of the spin vector, given by (2.2.33), and this is equivalent to an  $\mathbf{L} \cdot \mathbf{S}$  coupling, so that the effective attractive potential becomes

$$V_{\text{eff}} = V(r) - \frac{1}{2m_s^2c^2} \left( \frac{1}{r} \frac{dV}{dr} \right) \mathbf{L} \cdot \mathbf{S} \tag{13.5.9}$$

where  $m_s$  is the strange-quark mass. Now, since  $-(1/r)dV/dr$  is negative,  $|V_{\text{eff}}|$  will be largest if  $\mathbf{L} \cdot \mathbf{S}$  is positive. Hence the binding takes place

preferentially when  $\mathbf{S}$  is parallel to  $\mathbf{L}$ , i.e. opposite to the normal to the scattering plane  $\mathbf{n} = \mathbf{p} \times \mathbf{p}_\Lambda$ . Thus the  $\Lambda$ s are produced preferentially with spin opposite to  $\mathbf{n}$ , i.e. are negatively polarized as required. The model also predicts that  $|\mathcal{P}_\Lambda| \propto p_T$  as is seen experimentally.

An interesting prediction arises in the case of  $K^-p \rightarrow \Lambda X$  for the  $\Lambda$  in the  $K^-$  fragmentation region. Now the  $s$  quark is initially in the  $K^-$  and moving too fast, so must decelerate to form the  $\Lambda$ . The Thomas precession is now reversed and  $\mathbf{S}$  along  $\mathbf{n}$  is favoured. Indeed the  $\Lambda$  polarization is found to be positive in this reaction, though its magnitude is twice as large as in  $pp \rightarrow \Lambda X$  and this is not explained by the model.

Nor can the model explain the differing behaviours of the various antihyperons; see (13.5.5) and (13.5.6).

### 13.5.3 Concluding remarks

For access to the detailed literature and for a description of some other phenomenological models the reader is referred to Soffer (1999).

In summary, it has to be admitted that there is still, after 25 years of experiment and some decades of QCD, no coherent theory of the hyperon polarization data. Moreover the richness of the experimental data is continually growing, and none of the models can explain the beautiful discovery by the E704 experiment of Fermilab (Bravar *et al.*, 1995; 1997) that the analysing power  $A_N$  and the spin-transfer parameter

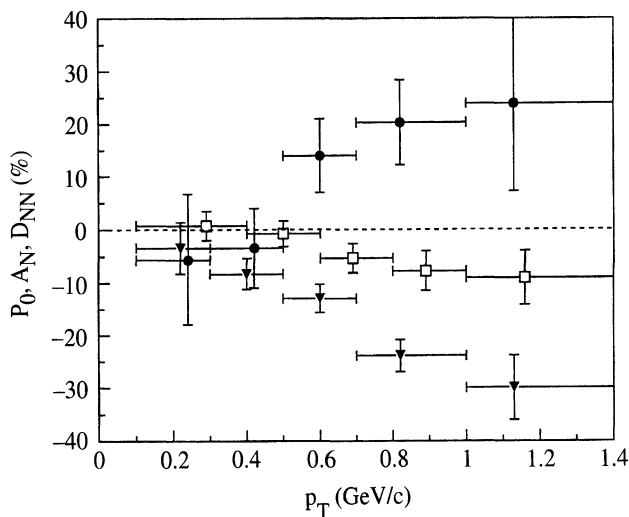


Fig. 13.21 Fermilab E704 data on  $\Lambda$  polarization  $P_0$  (triangles), analysing power  $A_N$  (squares) and spin-transfer parameter  $D_{NN}$  (circles), each given as a percentage, for  $pp \rightarrow \Lambda X$  at 200 GeV/c. (Courtesy of A. Penzo.)

$D_{NN}$  are both large and growing with  $p_T$  in  $pp \rightarrow \Lambda X$  at 200 GeV/ $c$  (see Fig. 13.21).

This whole area of high energy physics remains an open challenge to the theory of strong interactions.